Habitat use by *Gadiculus argenteus* (Pisces, Gadidae) in the Galician and Cantabrian Sea waters (NE Atlantic)

Juan C. Arronte[1],*, José M. González-Irusta[1], Raquel Somavilla[1], Juan Fernández-Feijoo[2], Santiago Parra[2], Alberto Serrano[1]

[1]**Instituto Español de Oceanografía, C. O. de Santander, 39004 Santander, Spain**
[2]**Instituto Español de Oceanografía, C. O. de A Coruña, 15001 A Coruña, Spain**

ABSTRACT: Forage fish species play a crucial role in most ecosystems, transferring energy from plankton to larger fishes. Therefore, understanding the factors driving the dynamics of forage fish populations is essential in marine ecosystems. *Gadiculus argenteus* is an important forage fish species in the Galicia and Cantabrian Sea ecosystem. In this study, the influence of several biotic and abiotic factors on the distribution of this species was examined using generalized additive models in a 2-step approach. *G. argenteus* habitat preference was not affected by changes in annual abundance during the study period (1998–2019). From the variables selected in the final models, depth and geographic location (latitude and longitude) were the most important factors to describe the presence of *G. argenteus*. Peak abundance was found on the upper slope and although the species was found throughout the study area, its higher abundance values were located in Galician waters. The species seemed to avoid coarse sand bottoms, with mean chlorophyll *a* concentration showing a positive effect on the presence and abundance of *G. argenteus*. Interestingly, the observed aggregations of *G. argenteus* showed a remarkable similarity to the commercial trawling footprint in the area, suggesting a strong link between the distribution of this forage species and the distribution of its predators, most of which are important commercial species. Further work should focus on a better understanding of this relationship to provide important information on the study of the structure and functioning of the marine ecosystem of the northern Spanish continental shelf.

KEY WORDS: Distribution models · Habitat · *Gadiculus argenteus* · Forage fish · Generalized additive model · Northeast Atlantic Ocean

1. INTRODUCTION

Fish populations are not distributed randomly in space but exhibit spatial patterns. Understanding which factors drive these patterns of spatial distribution is both a fundamental ecological need and a requirement for resource management and marine spatial planning (Planque et al. 2011). This is especially true in the current context of implementation of the ecosystem approach in the management of marine ecosystems and its reflection in legislation bodies

worldwide (Enright & Boteler 2020). In the case of forage fish species, unravelling the factors driving their spatial distribution is even more important, since it is not only a key issue in the study of the structure and functioning of marine communities and ecosystems, but it is also very useful for developing ecosystem models (Bailey et al. 2010). Forage fish occupy central positions in marine food webs by feeding on zooplankton and acting as primary prey for larger fish, marine mammals and seabirds (Van der Lingen et al. 2009). Due to their key role in the

ecosystem linking bottom-up and top-down processes (Lynam et al. 2017), a better understanding of the distribution and the environmental factors which define the distribution of forage species will help to predict future adaptive responses of the ecosystem to a change in external drivers such as fishing or climate change (Lindegren et al. 2018, Régnier et al. 2019).

The marine food web of the northern continental shelf of Spain (NE Atlantic) shows a high diversity and complexity due to the large number of links between functional groups, with strong relationships between the pelagic, demersal and benthic domains, with forage fish playing a major role in the energy transfer from the pelagic to the demersal and benthic domains (Sánchez & Olaso 2004, Preciado et al. 2008, Corrales et al. 2022). In this trophic web, almost 40% of the global diet composition of demersal fishes consist mainly of 2 small bentho-pelagic fish species: blue whiting *Micromesistius poutassou* and southern silvery pout *Gadiculus argenteus* (Preciado et al. 2008, Rodríguez-Cabello et al. 2014). Yearly fluctuations in the abundance of these 2 forage species seem to affect the feeding ecology of their predators. Thus, an increase in cannibalism in *Merluccius merluccius* due to the scarcity of its main prey species, *Micromesistius poutassou* (Preciado et al. 2015) and a correlation between shifts in *G. argenteus* abundance and its importance in the diet of its predators, both in volume and frequency of occurrence (Rodríguez-Cabello et al. 2014), have been observed.

G. argenteus Guichenot, 1850 is a member of the family Gadidae inhabiting the deeper parts of the shelf and upper slope in warm-temperate latitudes of the NE Atlantic (between 20° N and 45° N) and the Mediterranean Sea (Gaemers & Poulsen 2017). It is a short-lived species (3–4 yr) (Gaemers & Poulsen 2017), and off the northern coast of Spain, it feeds on various groups of small pelagic and benthopelagic crustaceans such as euphausiids and natantians (López-López & Preciado 2015). Due to its schooling behaviour, broad geographic distribution, high relative abundance and small size (L_{max} = 15.0 cm, Gaemers & Poulsen 2017), *G. argenteus* is an important trophic resource for non-commercial such as *Lepidopus caudatus* and *Molva macrophtalma* and for many commercial species such as hake *Merluccius merluccius*, megrims (*Lepidorhombus* spp.), anglerfishes (*Lophius* spp.) and *Micromesistius poutassou*, among other species (Gutiérrez-Zabala et al. 2001, Preciado et al. 2008, Rodríguez-Cabello et al. 2014 and references therein).

Despite the relevance of *G. argenteus* in the trophic ecosystem dynamics of the Spanish northern continental shelf, there is not only little detailed information on its biology but also a general lack of knowledge on the ecological preferences of the species. To address the need to understand the relationship between species distributions and the physical environment, a wide variety of numerical techniques encompassed under the term 'distribution models' (DMs) have been developed during the last decades (Elith & Leathwick 2009). According to those authors, a DM is a model that relates species distribution data (occurrence and/or abundance at known locations) with information on the environmental and/or spatial characteristics of those locations. Among the different DM methods, generalized additive models (GAMs) (Hastie & Tibshirani 1990) have been successfully used to model the spatial distribution and environmental preferences of marine fish species (e.g. Maravelias et al. 2007, Sagarese et al. 2014, González-Irusta & Wright 2016a,b, Mbaye et al. 2020).

The use of long-term fish data can be a valuable tool in describing fish habitats (Feyrer et al. 2007); Spanish long-term monitoring surveys offer an exceptional opportunity to model the occurrence of *G. argenteus* using data from a fishery-independent multispecies bottom-trawl survey. The aims of this study were (1) to determine the importance of environmental factors on the distribution of *G. argenteus* on the Spanish northern continental shelf, and (2) to map, for the first time for the species, its spatial distribution and relative biomass. In the present study, we explore the environmental variables that influence the spatial distribution of *G. argenteus* using data from a historical series of research surveys together with a suite of biotic and abiotic factors and applying a 2-step GAM. In an area experiencing climate warming (Somavilla et al. 2017), improving knowledge about the environmental drivers and spatial distribution of *G. argenteus* is necessary, for example, to understand the effect that significant variations in the biomass and/or distribution of the species could cause in the food web, to increase our current understanding of marine ecosystem functioning, and to help in forecasting ecosystem resilience and adaptability to different scenarios of climate change.

2. MATERIALS AND METHODS

2.1. Study area

The study area comprises the northern Spanish shelf (southern Bay of Biscay, NE Atlantic) (Fig. 1). It is located at temperate latitudes, and the orientation
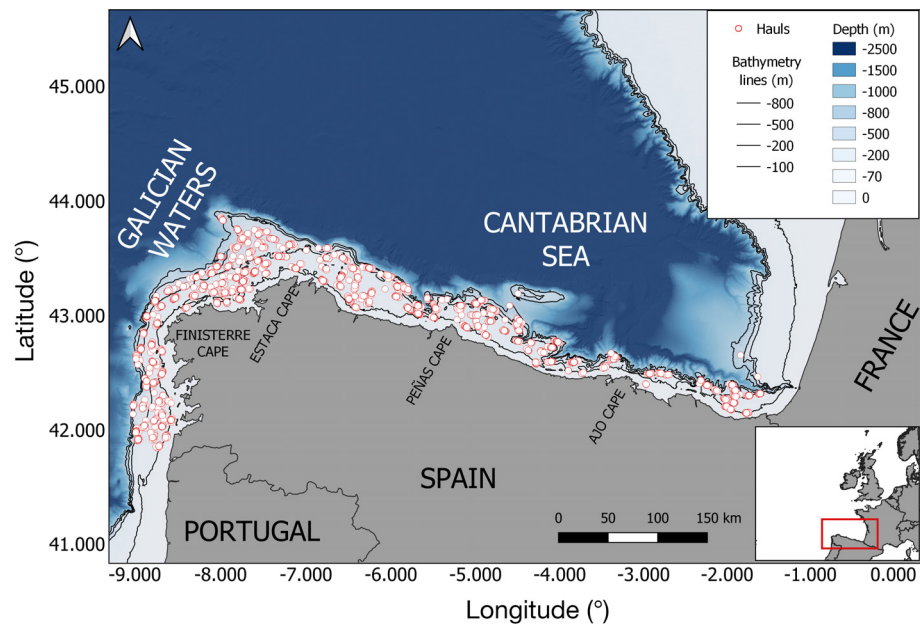
Fig. 1. Study area with the distribution of the hauls carried out during the study period (1998–2019)

of the coastline, south–north up to Cape Finisterre, then turning northeastwards towards Cape Estaca de Bares and finally running west–east in the Cantabrian Sea, has a great influence not only on the oceanography but also in the ecosystem dynamics of the area. Thus, 2 different areas with different sedimentary and hydrographic characteristics can be recognized: the Galician waters (ICES Division IXa) and the Cantabrian Sea (ICES Division VIIIc). The Galician waters are the northern edge of one of the major upwelling areas in the world, the eastern boundary system off NW Africa and SW Europe (Wooster et al. 1976). The frequent and seasonal upwelling of cold and dense North Atlantic Central Water (NACW) results in nutrient enrichment of the area, which ensures elevated primary production and high ecosystem productivity (Figueiras et al. 2002). The intensity of the upwelling decreases towards the Cantabrian Sea, and in this area, the dynamic of the ecosystem is greatly determined by seasonality, with a regular pattern of hydrographic conditions throughout the year characterized by winter mixing and summer stratification, with phytoplankton blooms occurring during the transition periods (Sánchez & Gil 2000).

Regarding seabed characteristics, the Galician shelf comprises a narrow strip (30 km wide from the coast) with rocky outcrops mainly located on the inner shelf and with 2 provinces: north and west of Cape Finisterre with the shelf essentially covered by a blanket of sand, and the area south of the Cape (where the coastline is characterized by the presence of many sea-drowned valleys known as 'Rías' and

the large Miño River) with muddy bottoms on the inner shelf and sandy bottoms in the middle and outer shelf (López-Jamar et al. 1992, Fernández-Salas et al. 2015). For its part, the Cantabrian Sea is cut by many submarine canyons, the shelf is very narrow (4–25 km wide), with rocky outcrops patchily distributed and a steep slope (Fernández-Salas et al. 2015). Moreover, the area west of Cape Peñas is wider and sandy, whereas the eastern area is narrower and muddier. In general, muddy sediments are located on the edge of the shelf and slope, and, due to the discharge of French rivers, on the shelf of the easternmost part of the Cantabrian Sea (Rey & Medialdea 1989).

2.2. Fish data

We used data collected during the DEMERSALES bottom trawl surveys (ICES code: SPGFS WIBTS-Q4) carried out annually every autumn (September–October) along the trawlable bottoms of the northern continental shelf of Spain for demersal fishery and benthic ecosystem assessment. These surveys are based on a stratified random sampling design with trawling operations carried out during daylight and the sampling unit made up of 30 min hauls at a speed of 3.0 knots, using a baca 44/60 otter trawl gear (Sánchez 1993). The survey area was stratified according to depth and bio-geographical criteria in 3 depth strata (70–120, 121–200, 201–500 m) and the number of hauls per stratum is proportional to the surface area available for trawling in each strata.

Furthermore, additional hauls shallower than 70 m and deeper than 500 m are performed every year whenever possible. The methodology used in these surveys remained unchanged throughout this historic series (ICES 2017). We used biomass data from all 2814 valid hauls carried out from 1998 to 2019 (see Tables S1 & S2 in the Supplement at www.int-res.com/articles/suppl/m694p175_supp.pdf). Biomass was expressed in terms of total weight (kg) of *Gadiculus argenteus* captured in each haul.

2.3. Environmental data

In this work we used 2 types of environmental information: environmental data which did not show relevant variation across the studied period: depth, slope and sediment type; and environmental data which showed important variations among years: near-bottom temperature, near-bottom salinity and chlorophyll *a* (chl *a*) (mean and maximum concentration, the day when the maximum occurs and the relative anomaly; see later in this section for a detailed explanation). All layers were constructed in R v.3.6.3 (R Core Team 2020) to a final resolution of 3 × 3 km, computing 1 unique layer for the constant variables (Fig. S1) and 1 layer by year for the other variables (Figs. S2–S7).

The bathymetry layer (Fig. S1) was obtained using data from the European Marine Observation and Data Network (EMODnet) Bathymetry portal (www.emodnet-bathymetry.eu/) and projected to the final resolution using a bilinear interpolation with the function 'projectRaster' from the R package 'raster' (Hijmans 2021). The processed bathymetry layer was then used to produce the slope layer using the 'terrain' function in the package 'raster' (Hijmans 2021). From 2014 to 2019 and during the DEMERSALES surveys, a total of 558 sediment samples were collected from the study area using a box-corer. Prior to analysis, samples were oven-dried at 100°C and then 5 ml of sodium polyphosphate and distilled water were added to disaggregate the sediment particles. The particle size distribution of the samples was analysed using a laser-diffraction-size analyser. The instrument provided grain size statistical parameters, including median particle diameter (Q50, µm) and sorting coefficient (So). The percentage of organic matter (%OM) content of the sediment was quantified as weight loss of dried (100°C, 24 h) samples after combustion (450°C, 24 h). Samples were classified into 3 sedimentary types according to the relative abundance of the particle size classes: mud (<62 µm), fine sand (62–500 µm) and coarse sands (>500 µm). Then, the sediment and the organic matter layers were generated to the final resolution interpolating the box-corer samples with the function 'fit.gstatModel' from the 'GSIF' package (Hengl 2019). The DEMERSALES survey only samples soft bottoms, and due to the presence of several rocky outcrops in the study area (Fernández-Salas et al. 2015), rock data were downloaded from the EMODnet Geology portal (www.emodnet-geology.eu) and areas with rocky substrates were erased from the sediment and organic matter layers prior to the inclusion of these 2 layers in the models. Therefore, the models predictions only covered soft bottom areas, and the distribution of *G. argenteus* on rocky areas was not analysed in this work.

Near-bottom temperature and salinity were calculated using CTD data from samples taken concurrently with the hauls. For each CTD profile, the deepest value of temperature and salinity was extracted. The near-bottom temperature and salinity values were then interpolated to the final resolution using regression kriging (with depth as a covariate) using the implementation 'fit.gstatModel' from the 'GSIF' package (Hengl 2019) (Figs. S2 & S3).

The importance of biomass accumulation associated with near-surface phytoplankton blooms and its timing (phenology) has been largely recognized as crucial in the population dynamics of higher trophic levels and in global biogeochemical cycles (Somavilla et al. 2019). To identify the near-surface signal of the phytoplankton bloom and investigate the effects of its intensity and phenology on *G. argenteus*, weekly satellite-derived chl *a* concentration data at 22 × 22 km resolution provided by the GlobColour project (www.globcolour.info) were used. For each grid, the mean (chl_{mean}) and maximum chlorophyll concentration (chl_{max}) and the day when it occurs (D_{max}) every year during the climatological period of the spring bloom in the area (March, April and May) was obtained. A fourth index (relative anomaly, AD_{max}) representing how much earlier or later the D_{max} occurs every year at each particular location with respect to its climatological value was calculated as:

$$AD_{max} = D_{max} - D_{clim} \qquad (1)$$

where D_{max} is for each particular grid and year, and D_{clim} is the climatological value of D_{max} at this particular grid (e.g. AD_{max} = +10 indicates a delay of the spring bloom of 10 d). All the chlorophyll layers (Figs. S4–S7) were projected to the final resolution using a bilinear interpolation.

The values of all the environmental variables included in the analysis were obtained using the location of the hauls, estimated as the mean point between the shoot (defined as the moment when both the vertical net opening and doorspread are stable) and haul (defined as the start of pulling the net back in) positions (ICES 2017), to extract the value at this point from the environmental layer.

2.4. Geostatistical aggregation curves

To establish the type of spatial dynamics of *G. argenteus* during the study period, geostatistical aggregation curves and the space selectivity index (Ssp) (Petitgas 1998) were calculated for every year. The curves show the proportion of total biomass (P) per area unit (T_z), which in the present study was the kg per haul of *G. argenteus*, as a function of the proportion of hauls (used in this work as a proxy for area) occupied by *G. argenteus* biomass. A complete description on how to calculate geostatistical aggregation curves can be found in Petitgas (1998). The aim of the Ssp is to differentiate between different spatial dynamics, providing information about the level of aggregation of the species. Ssp was calculated following the formula proposed by Tamdrari et al. (2010), and differences in the Ssp index between years were tested using bootstrapping (Petitgas 1998). Thus, the original dataset (for all the years together) was randomly resampled 1000 times with replacement. The P-curves were then recalculated for the new dataset, and the mean Ssp and 95 % confidence intervals were calculated using the 'boot' and 'boot.ci' functions from the 'boot' package (Canty & Ripley 2021) in R. If the annual Ssp value for one of the years was outside the confidence interval, the null hypothesis (no significant variation in Ssp among years) was rejected.

2.5. Data analysis

Statistical analyses were carried out in R v.3.6.3 (R Core Team 2020). The biomass of *G. argenteus* along the study area was modelled using GAMs. Since the data was zero-inflated, the spatial distribution was modelled using a 2-stage model (delta method) (Barry & Welsh 2002). This 2-step modelling was used as an attempt to deal with the difficulties of modelling over-dispersed data (Zuur et al. 2009), as is frequently the case with bottom trawl surveys. Two-step models have been successfully applied to

model the spatial distribution of fish habitats (e.g. Loots et al. 2011, Sagarese et al. 2014, González-Irusta & Wright 2016a,b, 2017).

First, the probability of presence (P_p) was modelled using a logit link and a binomial error distribution. Then, the biomass of *G. argenteus* (calculated for 30 min of trawling and removing the zeros) was log-transformed and modelled using an identity link and a Gaussian error distribution. In both models, all the smoothers were constrained to 4 knots (the exception was the spatial effect, which was constrained to 16 knots) to avoid overfitting (Guntenspergen 2014). All GAMs were built with the implementation 'gam' in the package 'MuMIn' (Bartoń 2020) and the optimal (best-fitting) model was chosen based on the lowest Akaike's information criteria (AIC) value. Finally, both models were combined to produce the final delta models (see Section 2.6). Delta models are the final prediction, combining the P_p of *G. argenteus* with the predicted biomass (P_b) by multiplying both outputs.

Before starting the analyses, the correlation between the explanatory variables was checked for collinearity using Spearman's rank correlations and variance inflation factors (VIFs) (Zuur et al. 2009). If large correlations between any 2 variables occurred, i.e. Spearman's rank coefficients >0.7 (Dormann et al. 2013) and VIF ≥3 (Zuur et al. 2009), one of the variables was excluded to minimize collinearity. Thus, chl_{max}, D_{max} and fine sand were removed. These variables were dropped based on the biology of the species. After these changes, the Spearman and VIF values of the remaining variables were lower than their thresholds, so all the other variables were included in the models. Finally, in order to consider other potential spatial effects produced by unmeasured drivers that could cause spatial autocorrelation in the residuals, the location of each trawl (longitude and latitude) was included in the model year by year. The full binomial model was:

$$
\begin{aligned}
P_p = &\ \beta_1 + s_1(depth) + s_2(salinity) + \\
&\ s_3(temperature) + s_4(mud) + s_5(coarse\ sand) + \\
&\ s_6(organic\ matter) + s_7(mean\ chlorophyll) + \quad (2)\\
&\ s_8\,(chlorophyll\ anomaly) + s_9(longitude, \\
&\ latitude,\ by = f(year)) + f_1(year) + \varepsilon_1
\end{aligned}
$$

where P_p is of *G. argenteus*, β_1 is the intercept, s is an isotropic smoothing function (thin-plate regression splines), f indicates the variables which were included as factors and ε_1 is the error term. The P_b of *G. argenteus* was modelled including the same variables as in the binomial model. The relative importance of each variable was tested by removing the targeted variable

from the final model and computing the deviance variation. The spatial autocorrelation of deviance residuals was analysed for each year and modelled separately using Moran's I correlogram, applying the function 'moran' from the 'spdep' package (Bivand et al. 2013). As the p-values were not statistically significant in any year for any model, the spatial autocorrelation in the residuals was considered nil.

2.6. Combining the delta maps

The prediction of aggregations of the 22 yr was combined in 1 unique final map, following Colloca et al. (2009) and González-Irusta & Wright (2017). Applying their methodology, the delta maps were converted to binary maps using an abundance threshold for each year. Using geostatistical aggregation curves, we defined the yearly thresholds at the point where a tangent line to the curve had a 45° slope. According to those authors, this point corresponds to a change in the spatial distribution of fish from a dispersed distribution pattern to an aggregated pattern. A more complete description of the methodology can be found in Colloca et al. (2009). Once the 22 maps were converted to binary maps, the index of persistence (I_i) was computed as:

$$I_i = \frac{1}{n} \sum_{k=1}^{n} F_v \qquad (3)$$

where n is the number of years considered and F_v is the value of each cell. F_v varies between 1 (the cell is considered suitable for aggregation) if the P_b in this cell was higher than the corresponding threshold, and 0 otherwise (i.e. the cell is not considered suitable for aggregation). I_i ranges between 0 (cell i never had a value higher than the threshold) and 1 (cell i always had a value higher than the threshold) for each cell in the study area. The I_i allows us to show 1 unique map with the distribution of *G. argenteus* in the study area.

2.7. Evaluating the models

The accuracy of the 3 models was tested using cross-validation. Since spatial data mostly have a local bias, spatial autocorrelation must be avoided between training and test data to make estimation model suitable for the entire, and not only for a specific local region of the dataset (Meyer et al. 2018). Therefore, it is essential that partitioned spatial data should be composed evenly over the entire region.

This objective can be achieved by following a spatial cross-validation strategy (Roberts et al. 2017). In the present study, spatial cross-validation was carried out using a checkerboard strategy, applying the function 'spatialBlock' from the R package 'blockCV' (Valavi et al. 2019) to divide the data into training and testing sets using spatial blocks. The size of the spatial blocks (near 25 km) was decided by using the function 'spatialAutorange' from the same package, which basically allows us to use the range of the spatial autocorrelation in the explanatory variables to determine the size of the spatial blocks. Then, data present in each group of blocks (see Valavi et al. 2019 for a further description of the checkerboard strategy) was randomly assigned as test or training data. Finally, each training and data set were randomly subsampled selecting 80 % of the data of each set in each iteration to avoid getting exactly the same data. The operation was repeated 10 times and in each iteration a set of evaluation metrics was computed. The predictive power of the presence–absence model was evaluated by calculating the area under the curve (AUC) (Fielding & Bell 1997), the kappa value (Cohen 1960) and the true skill statistics (TSS) (Allouche et al. 2006). The AUC provides a measure of the model's ability to predict presences as presences and absences as absences. The value of AUC varied from 0 to 1; ≤0.5 suggests that the model has no predicting capability, while ≥0.7 indicates that the model is acceptable (Hosmer et al. 2013). Kappa corrects the overall accuracy of model predictions by the accuracy expected to occur by chance and its value ranges from −1 to +1, where +1 indicates perfect agreement, a value ≤0 indicates a performance no better than random and a value >0.4 is considered an acceptable measure of accuracy (Landis & Koch 1977). The TSS is a measure of specificity (proportion of correctly predicted absences) and sensitivity (proportion of correctly predicted presences) in the form of TSS = (specificity + sensitivity) – 1. TSS values range from −1 to 1, where 0 indicates no predictive power and a value ≥0.4 is considered a useful measure of accuracy (Zhang et al. 2015). The correlation between observed and predicted biomass values was evaluated using Spearman's rank correlation for both biomass and delta models. Spearman's rank values range from −1 to +1, where a complete absence of correlation is represented by 0 and an absolute value ≥0.4 is considered as the threshold for an acceptable correlation (Fowler et al. 1998). The process was repeated 10 times for each, with a different random selection of training and test subsample each time. The evaluation metrics were calculated applying the functions 'evaluate' from the R package 'dismo'

(Hijmans et al. 2020), 'cor' in the package 'stats' (R Core Team 2020) and 'Kappa' in the 'SDMTools' package (VanDerWal et al. 2014).

3. RESULTS

Yearly geostatistical aggregation curves and associated Ssp values along with the mean value and confidence interval for the period 1998–2019 are shown in Fig. 2. During this period, Ssp for all years was inside the correspondent confidence interval, and therefore, the null hypothesis of no significant variation of Ssp among years was accepted. Combined analysis of the aggregation curves and Ssp values indicates that the spatial dynamics of *Gadiculus argenteus* during the study period corresponds to Dynamic D2: 'consistent spatial pattern', i.e. where local fish density changes at the same rate as population abundance (Petitgas 1998, Tamdrari et al. 2010).

The binomial model explained 45.0% of the deviance (Table 1). From the 10 initial model variables included in the full binomial model, only %OM and chlorophyll anomaly were not kept in the final model. Depth was clearly the most important variable in the final model (Δ deviance = 288.48) (Table 1), showing that *G. argenteus* were most likely to be encountered at depths between 250 and 350 m (decreasing with shallower and deeper depths) (Fig. 3a). Mud was the least important variable (1.78), and sediment associations were found with coarse sand (negative association) and mud (positive association) contents (Fig. 3b,c). The P_p of *G. argenteus* increased with increasing values of mean chl *a* and slope (Fig. 3d,e). Salinity values higher than 35.7 and temperature values around 13°C increase the chance of species encounter (Fig. 3f,g). The inter-annual variation of the coefficient values did not show any clear temporal trend, with the higher probability of occurrence in 2001 and the lower in 2012 (Fig. 3h). Although year, salinity and mud did not have a statistically significant effect on P_p (Table 1), they were left in the final model, as removing these variables deteriorated both the AIC score and the deviance
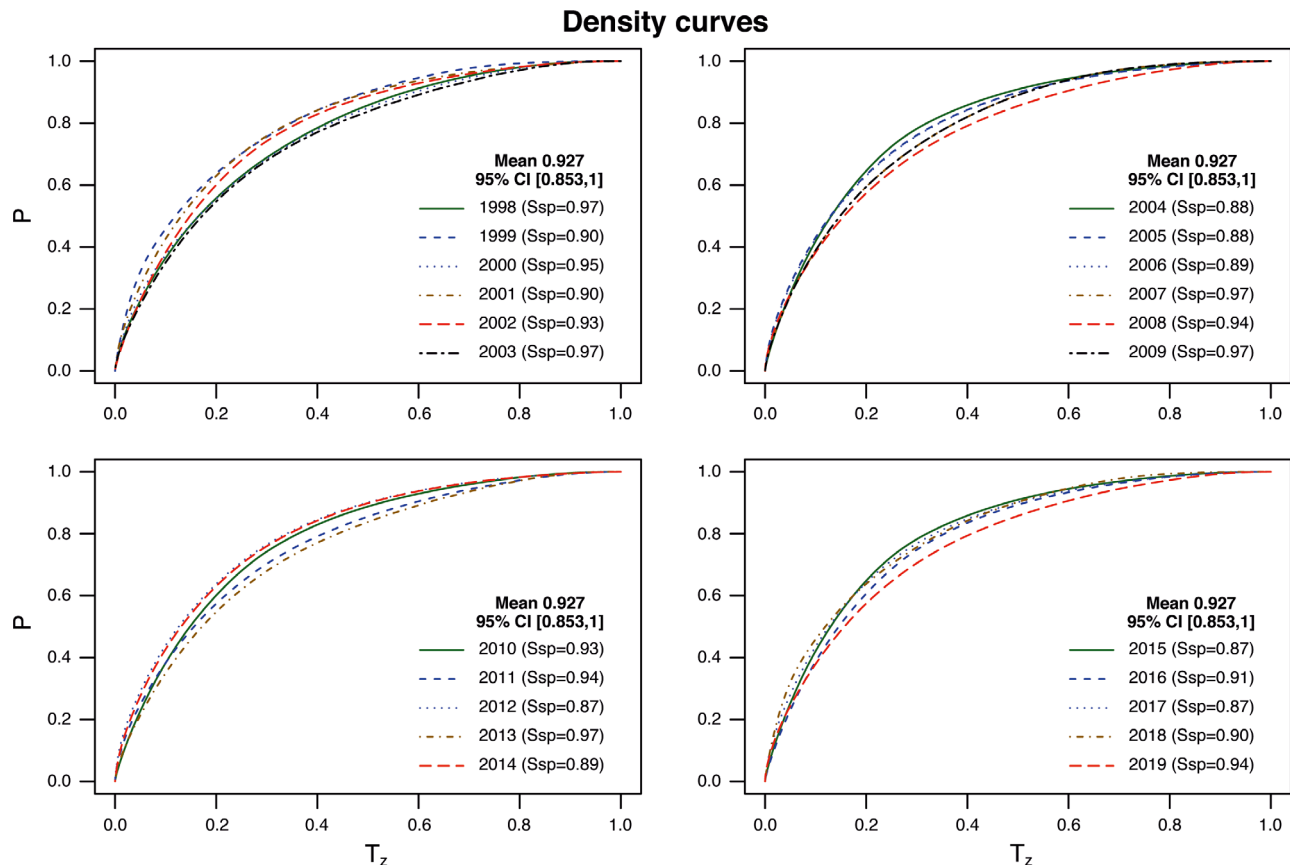
Density curves

Fig. 2. Annual geostatistical aggregation curves and space selectivity index (Ssp) values for *Gadiculus argenteus* abundance for the study period (1998–2019). The curves relate the proportion of total biomass (P) per surface unit (T_z). Mean, 95% confidence intervals (in square brackets) and annual values (in parentheses) of Ssp are shown for the whole study period. Data is displayed in 4 panels for better readability

Table 1. Number of hauls (N), relative importance (Δ deviance), degrees of freedom (df) or estimated degrees of freedom (edf) and statistical significance (p-value) of the explanatory variables for the presence−absence (binomial) model

Model		N	Explained deviance
Binomial		2814	45.0%
Parametric terms	Δ deviance[a]	df/edf	Chi	p
Year	6.13	21	32.0	0.068
Smoother terms	153.77			
Spatial effect 1998		2.69	0.65	0.921
Spatial effect 1999		6.70	15.52	0.075
Spatial effect 2000		9.46	18.74	0.091
Spatial effect 2001		9.72	23.14	0.052
Spatial effect 2002		4.67	13.53	<0.050
Spatial effect 2003		6.09	20.74	<0.010
Spatial effect 2004		5.30	6.64	0.469
Spatial effect 2005		9.63	20.95	<0.050
Spatial effect 2006		6.54	19.73	<0.050
Spatial effect 2007		2.38	5.54	0.076
Spatial effect 2008		5.88	25.04	<0.010
Spatial effect 2009		2.39	10.71	<0.010
Spatial effect 2010		5.87	16.42	<0.050
Spatial effect 2011		2.00	4.29	0.114
Spatial effect 2012		4.22	7.55	0.227
Spatial effect 2013		2.00	23.01	<0.001
Spatial effect 2014		2.00	18.66	<0.001
Spatial effect 2015		8.16	18.88	<0.050
Spatial effect 2016		8.68	28.62	<0.010
Spatial effect 2017		2.00	4.49	0.118
Spatial effect 2018		3.47	18.04	<0.010
Spatial effect 2019		2.78	9.69	<0.050
Depth	288.48	2.98	304.64	<0.001
Coarse sand	34.02	2.35	27.95	<0.001
Mean chlorophyll concentration	20.68	1.00	16.32	<0.001
Temperature	17.80	2.37	9.82	<0.050
Slope	7.59	1.00	11.83	<0.001
Salinity	2.31	1.53	5.45	0.091
Mud	1.78	1.00	9.11	0.073

[a]Deviance variation in the final model after elimination of the variable

because they improve the AIC value and increase the deviance explained by the final model. The spatial effect (Δ deviance = 209.16), depth (162.54) and year (102.11) were the 3 most important variables, whereas chlorophyll anomaly was the least important variable (1.51) (Table 2). P_b showed an increase with increasing depths up to 300 m depth and then a negative effect for deeper areas (Fig. 5a). Coarse sand showed a linear and decreasing trend, with highest biomass values in areas with no coarse sand (Fig. 5b). Biomass was higher at both low and high mud content (Fig. 5c). The effect of chl_{mean} on biomass was positive for values ranging from 0.3 to 2.0 mg m^{-3} and slightly negative for higher concentration values (Fig. 5d). Early chlorophyll blooms had a negative effect on P_b, whereas late blooms up to 10 d showed a positive effect and negative for higher values (Fig. 5e). There was an increase in the biomass of the species with increasing values of slope (Fig. 5f). Areas with a near-bottom temperature around 13.5°C were associated with high biomass values (Fig. 5g). *G. argenteus* biomass increased linearly with increasing salinity (Fig. 5h). The year coefficient did not show any specific trend, with the lowest coefficient in 2003 and 2013 and the highest in 2004 and 2005 (Fig. 5i). The spatial effect showed high inter-annual variability, especially in Galician waters, the area with the highest P_b during the study period (Fig. 6).

The yearly delta maps, which are the result of multiplying the presence/absence maps with abundance maps (biomass), showed that the main aggregations of the species are usually located in Galician waters, mainly between Cape Finisterre and Cape Estaca de Bares (Fig. 7). Moreover, aggregations on the upper slope south of Cape Finisterre have been found in some years. Finally, the distribution of I_i values, which range from 0 (the area was never predicted as being suitable for aggregation in all the years from 1998 to 2019) to 1 (the area was predicted to be suitable for aggregation all the years), is shown in Fig. 8. The persistent *G. argenteus* aggregations are mainly located in the deeper areas of the continental shelf and in the upper slope of the Galician waters. In the Cantabrian Sea, only 2 small areas consistently classified as suitable for aggregation were located: one in the west, which is actually the eastern end of the Galician aggregation, and the other in the centre of the Cantabrian Sea. In this latter area, the aggregations are restricted mainly to the upper slope.

Model evaluation outcomes are shown in Table 3. The P_p model showed AUC, kappa and TSS values higher than the threshold criteria for a good perform-

explained. The spatial effect (longitude and latitude of the haul by year) was the second most important variable (153.77). During the study period, high temporal variability, especially in the Cantabrian Sea, was observed (Fig. 4). This area showed years with high P_p and others with low values. On the contrary, Galicia showed high P_p values in all years.

The Gaussian model fitted for biomass explained 47.0% of the deviance (Table 2). In this model, only %OM was not included in the final model. Of the 10 variables included in the final model, chl_{mean}, salinity and chlorophyll anomaly showed no significant effects on the P_b of *G. argenteus*. However, they were kept
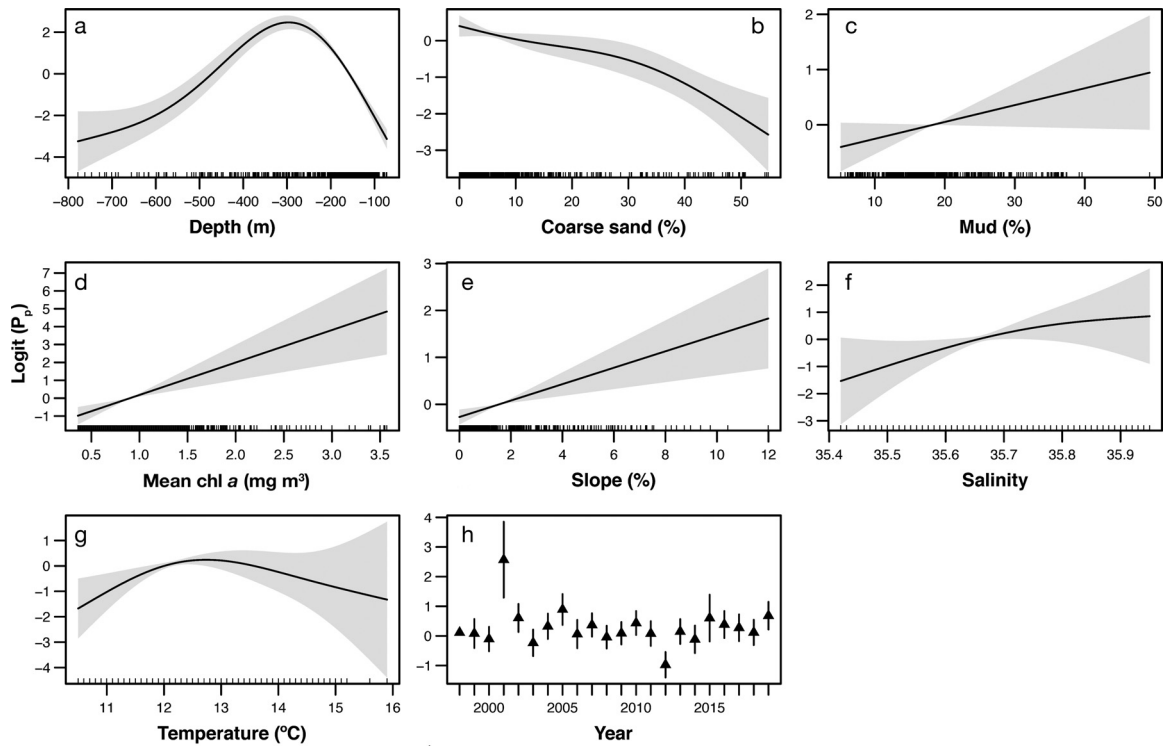
Fig. 3. Effect on the predicted probability of presence of *Gadiculus argenteus* (P_p) of the continuous explanatory variables (a: depth, b: coarse sand, c: mud, d: mean chl *a*, e: slope, f: salinity, g: temperature), and (h) coefficient value for the different levels of the explanatory variable 'year' which was included as factor. Shaded areas: 95% confidence intervals around response curves; error bars in (h): SD; rug plots: distribution of the observed values
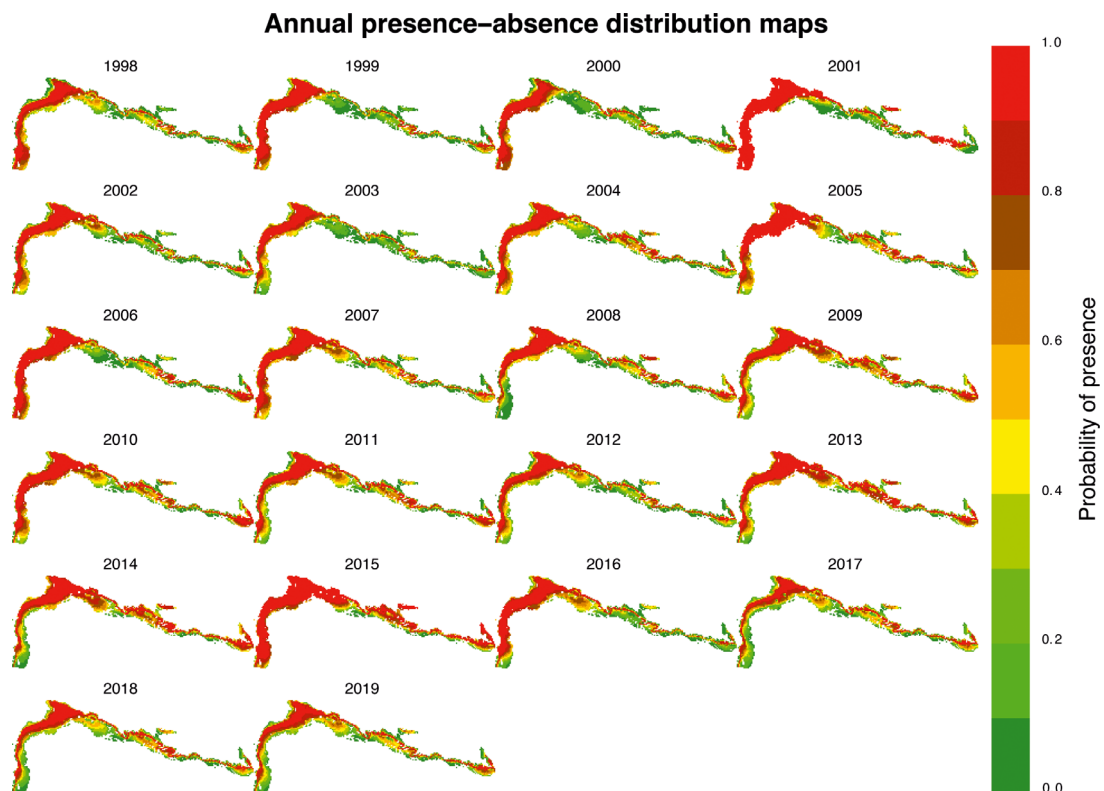
Annual presence–absence distribution maps

Fig. 4. Distribution maps of the probability of presence of *Gadiculus argenteus* (P_p) during the study period (1998–2019)

Table 2. Number of hauls (N), relative importance (Δ deviance), degrees of freedom (df) or estimated degrees of freedom (edf) and statistical significance (p-value) of the explanatory variables for the biomass (Gaussian) model

Model		N		Explained deviance
Gaussian		1793		47.0 %
Parametric terms	Δ deviance[a]	df/edf	F	p
Year	102.11	21	8.44	<0.001
Smoother terms	209.16			
Spatial effect 1998		4.86	1.66	0.118
Spatial effect 1999		2.04	3.53	<0.050
Spatial effect 2000		2.00	0.15	0.389
Spatial effect 2001		8.71	2.64	<0.050
Spatial effect 2002		2.00	4.70	<0.050
Spatial effect 2003		2.00	0.47	0.675
Spatial effect 2004		12.86	1.78	0.067
Spatial effect 2005		6.89	2.87	<0.010
Spatial effect 2006		8.34	3.05	<0.001
Spatial effect 2007		5.57	1.77	0.092
Spatial effect 2008		2.00	2.02	0.131
Spatial effect 2009		10.38	2.79	<0.001
Spatial effect 2010		3.42	1.16	0.323
Spatial effect 2011		8.55	2.98	<0.001
Spatial effect 2012		3.87	2.13	0.051
Spatial effect 2013		13.63	5.00	<0.001
Spatial effect 2014		5.72	1.00	0.437
Spatial effect 2015		10.88	2.57	<0.01
Spatial effect 2016		10.23	4.67	<0.001
Spatial effect 2017		3.65	3.18	<0.010
Spatial effect 2018		7.96	1.95	<0.050
Spatial effect 2019		7.14	2.25	<0.050
Depth	162.54	2.95	48.48	<0.001
Slope	10.88	1.37	24.15	<0.001
Coarse sand	9.69	2.45	8.05	<0.001
Mud	6.52	2.34	4.51	<0.010
Temperature	5.27	2.47	3.93	<0.010
Mean chlorophyll concentration	3.38	1.92	2.46	0.082
Salinity	2.17	1.00	1.27	0.284
Chlorophyll anomaly	1.51	1.97	0.63	0.426

[a]Deviance variation in the final model after elimination of the variable

ance, indicating that the model performs accurately. The Spearman coefficient value was 0.46 for the biomass model and 0.59 for the delta model, showing an adequate correlation between observed and predicted values in both models.

4. DISCUSSION

Using both a long time series from annual research surveys aiming at estimating demersal fish abundance and a 2-stage GAM, the present study has identified some of the biotic and abiotic mechanisms behind the spatial distribution in Galician and Cantabrian Sea waters of *Gadiculus argenteus*, an understudied forage fish species.

The 3 predictions (presence–absence, biomass in hauls with presence of the species and total biomass, delta model) showed good performance, comparable to, or even better than those of, similar fish distributional studies (e.g. Sagarese et al. 2014, González-Irusta & Wright 2017). These good model performances were probably obtained as a consequence of the intense coverage of the survey (both spatial and temporal) and the strong link between some of the tested environmental variables and *G. argenteus* distribution. The geostatistical aggregation curves suggest that during the study period, *G. argenteus* exhibited a proportional density population structure in which local abundance changes in proportion to changes in total species abundance. This is consistent with the proportional density dynamic model (D2) (Petitgas 1998) which is driven by a site-dependent mechanism (Petitgas 1998, Pereira et al. 2014), namely, the physical habitat preferences of the species during the period 1998–2019 were not modified by changes in its annual abundance. This spatial pattern has been previously observed in gadiforms in the eastern (e.g. Houghton 1987, Petitgas 1998, González-Irusta & Wright 2016a,b, 2017) and western North Atlantic (Tamdrari et al. 2010, Pereira et al. 2014).

Depth was the most important variable in the presence–absence model and the second most important in the biomass model. This was an expected result, since depth encompasses several crucial oceanographic factors for fish species, such as light, temperature, pressure or food availability, although disentangling the direct effect of these variables is frequently not possible. In the study area, depth is often the main gradient along which demersal fish species are organized on the shelf and upper slope (Sánchez 1993). In addition, bathymetry is a common descriptor of fish distribution among gadiform species globally (Howes 1991) and it was a good predictor of occurrence for other members of the Order Gadiformes in the NE Mediterranean (Pallaoro & Jardas 2002). In the northern Spanish continental shelf, the species has been commonly caught between 250 and 350 m depth (Sánchez 1993, the present study) and its higher abundance in the upper slope has been also observed in the Mediterranean Sea (Pallaoro & Jardas 2002, Damalas et al. 2010, Fernandez-Arcaya et al. 2013). Similar bathymetric distribution on the upper slope and the deeper parts
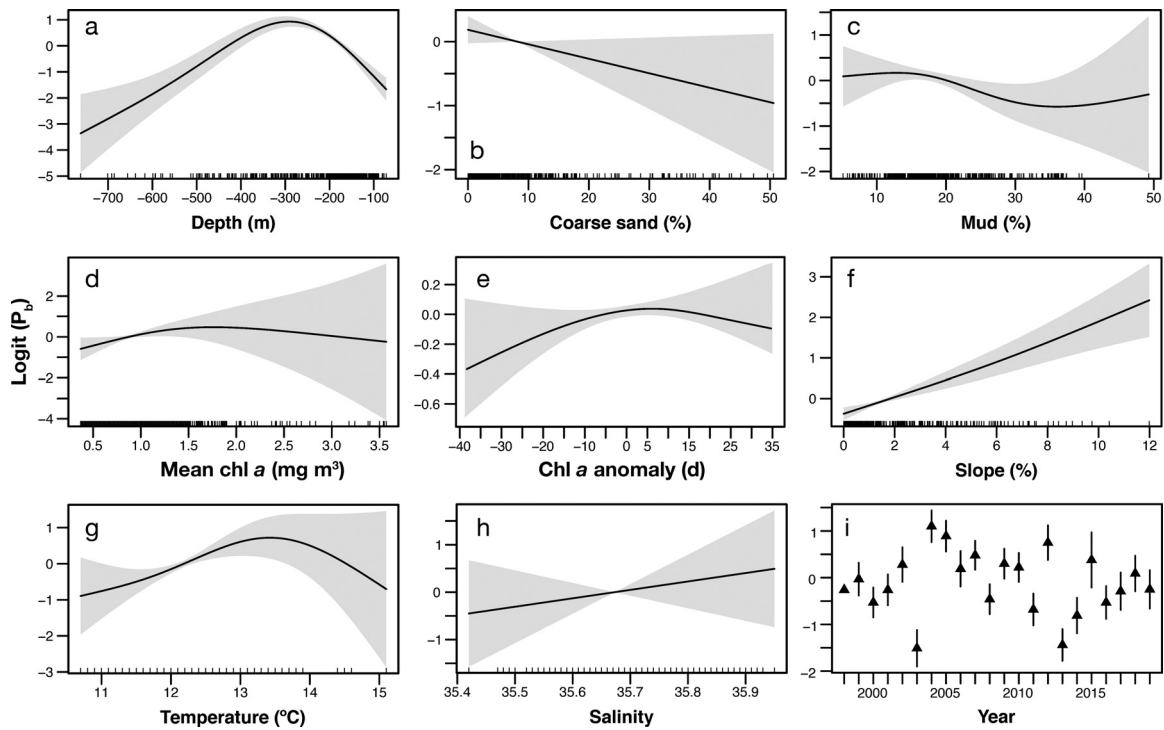
Fig. 5. Effect on the predicted biomass of *Gadiculus argenteus* (P_b) of the continuous explanatory variables (a: depth, b: coarse sand, c: mud, d: mean chl *a*, e: chl *a* anomaly, f: slope, g: temperature, h: salinity), and (i) coefficient value for the different levels of the explanatory variable 'year' which was included as factor. Shaded areas: 95 % confidence intervals around response curves; error bars in (i): SD; rug plots: distribution of the observed values

Annual biomass distribution maps
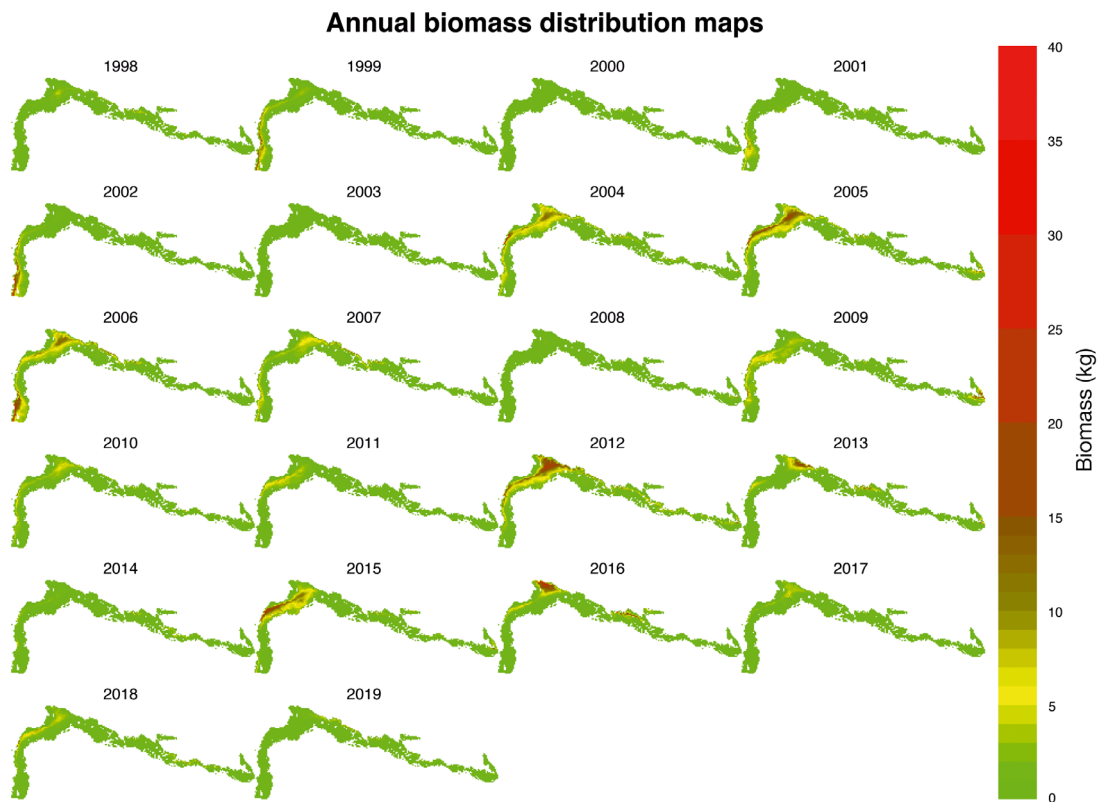
Fig. 6. Distribution maps of the biomass of *Gadiculus argenteus* in presence areas (P_b) during the study period (1998–2019)

Annual delta distribution maps
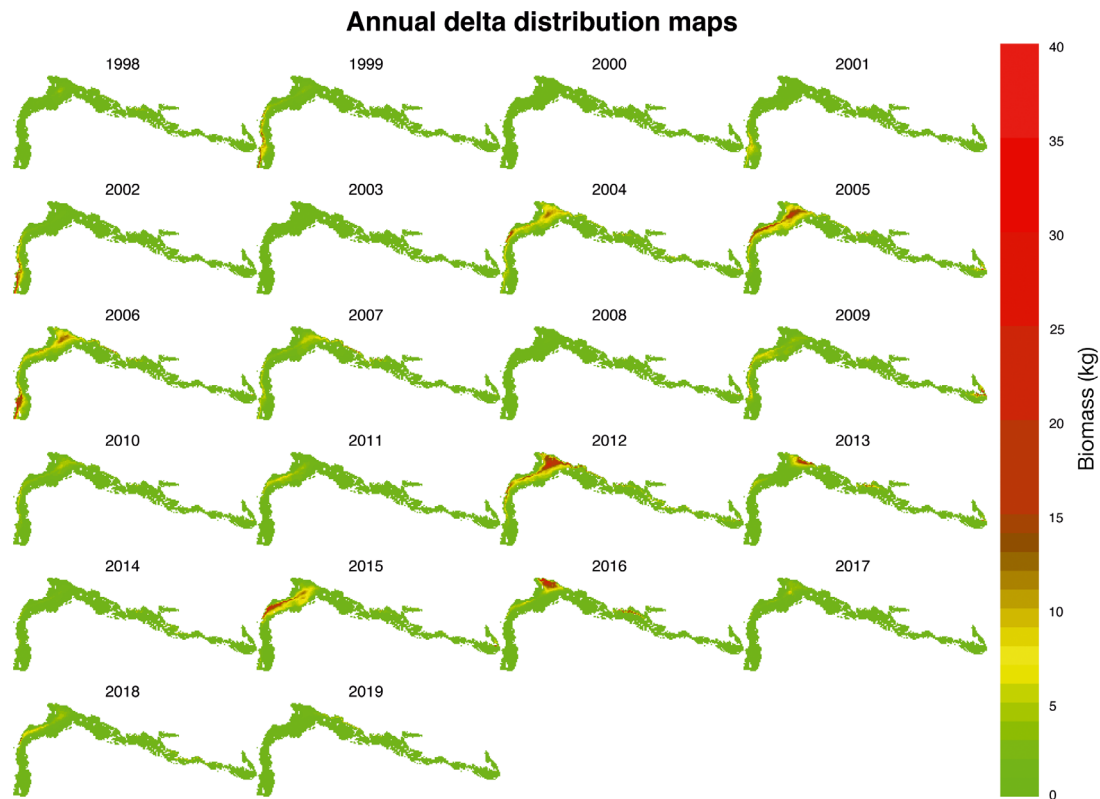
Fig. 7. Distribution maps of the biomass of *Gadiculus argenteus* in the delta model ($P_p \times P_b$) during the study period (1998–2019)
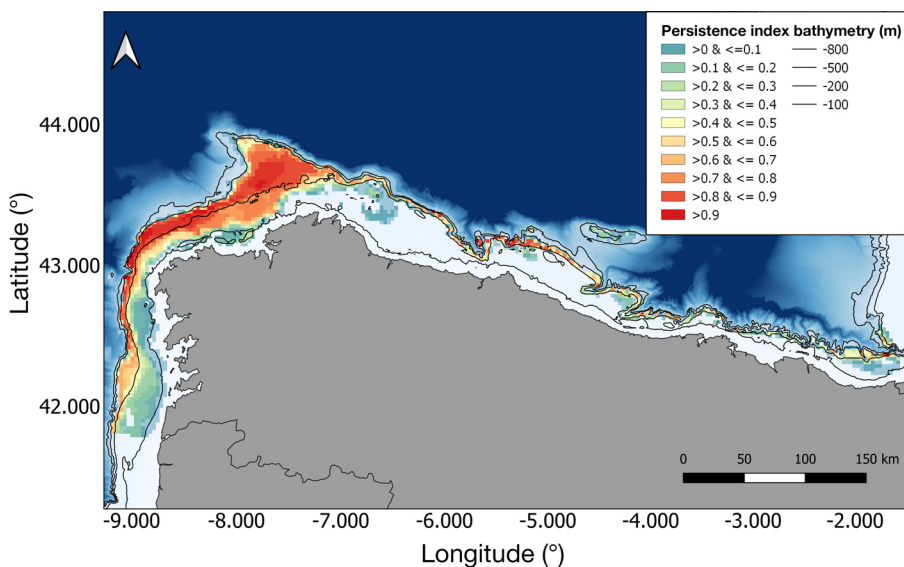

Fig. 8. Distribution of the index of persistence (I_i) of *Gadiculus argenteus* in the study area. I_i ranges from 0 (no aggregations found in any of the study years) to 1 (aggregations found in all of the study years)

of the continental shelf has been observed in its congener *G. thori*, although its highest catch rates are at shallower depths (150–300 m) (Hislop et al. 2015, Husson et al. 2020).

According to Cohen et al. (1990), *G. argenteus* aggregates over a wide range of substrates, from mud and muddy sand to gravel and rock bottoms.

However, according to Pallaoro & Jardas (2002), the species seemed to be absent from the rocky sediments of the western Mediterranean Sea. In the present work, the presence of *G. argenteus* over rocky bottoms cannot be ruled out due to the nature of the sampling carried out in Demersales surveys. Thus, the models of the present study refer to the popula-

Table 3. Evaluation outcomes (mean ± SD) for the probability of presence, biomass and the combined delta models. The probability of presence model was evaluated using area under the curve (AUC), kappa and true skill statistics (TSS). Biomass and delta models were evaluated by calculating the Spearman coefficient. na: not applicable

Model	AUC	Kappa	TSS	Spearman
Binomial model (Presence)	0.77 ± 0.04	0.47 ± 0.05	0.51 ± 0.04	na
Gaussian model (Biomass)	na	na	na	0.46 ± 0.02
Delta model	na	na	na	0.59 ± 0.04

tion thriving exclusively on soft bottoms, with rocky areas out of the scope of this work. Mud and coarse sand showed an inverse effect on the P_p of *G. argenteus*. However, while the trend between the percentage of mud and the abundance of the species was less apparent, the decrease in the biomass of the species with increasing values of coarse sand content seemed more evident. This apparent predisposition of *G. argenteus* to avoid coarse sand bottoms has been previously observed in the eastern Mediterranean Sea (Damalas et al. 2010). In the case of demersal fish species, the role of sediments in their spatial distribution has been related to the trophic interaction between fish species and their prey (Hinz et al. 2003). However, *G. argenteus* is a planktophagous species which, in the study area, feeds mainly on pelagic and benthopelagic crustaceans (López-López et al. 2017). Thus, its sediment preferences (Pallaoro & Jardas 2002, Damalas et al. 2010, the present study) might be related to current patterns in or near the sea bottom. Slow bottom currents favour the deposit of silt and fine sands (Brackenridge et al. 2018), and, at the same time, would allow pelagic and benthopelagic crustaceans to exhibit a normal vertical distribution pattern where their lower vertical limits can reach the sediment surface, making them available to benthopelagic fish species (Mauchline & Gordon 1991) such as *G. argenteus*.

Salinity along with bottom temperature showed a significative effect on *G. argenteus* distribution. In general, the species showed higher P_p and abundance in more saline waters with temperature values around 13.5°C. On the northern coast of Spain, these conditions are associated with the Iberian Poleward Current (IPC) and its intrusion into the Cantabrian Sea (the Navidad current) which transport these warmer and saltier waters along the coast (Somavilla et al. 2013). Interestingly, the distribution of these warmer and saltier waters in the continental shelf of the study area agrees with the higher abundance val-

ues observed in the delta models. On the other hand, the low abundance values observed in the muddy areas of the inner part of the Bay of Biscay could be related not only to the scarce penetration of the Navidad current in this area (Somavilla et al. 2013) but also to the influence of French rivers' freshwater discharge which would lead to colder and less saline waters. Salinity and temperature have not only been identified as some of the factors which explain the composition and structure of fish communities in the Cantabrian Sea (Sánchez & Serrano 2003) but also as key in the spatial distribution of mature (Hedger et al. 2004) and spawning gadoid species (González-Irusta & Wright 2016a,b, 2017). Temperature also plays an important role in the abundance and distribution of several zooplankton species exploited by *G. argenteus* (Lindley 1977).

The role that chl *a* plays in the body condition of gadiform species has been described (Rueda et al. 2015), but the present study is the first to provide information on the influence of primary production on their distributional preferences. Mean surface chl *a* concentration and chl *a* anomaly were included in the binomial and Gaussian final models respectively, showing their role not only on the presence but also on the spatial aggregation of *G. argenteus* on the northern Spanish continental shelf. High levels of chl *a* seem to indicate favourable conditions for the species, increasing both the P_p and the abundance of *G. argenteus*. Chl *a* concentration is generally accepted as an index of the standing stock of phytoplankton in surface waters (Longhurst et al. 1995). Since the main systematic groups of zooplankton feed on phytoplankton, high concentrations of chl *a* are likely to be associated with high food availability for a zooplanktivorous fish such as *G. argenteus*.

Our results show that changes in timing of the phytoplankton bloom have an effect on the biomass of *G. argenteus*. A change in the timing of the bloom may lead to trophic decoupling between phytoplankton and zooplankton (Edwards & Richardson 2004) and this mismatch may partly determine the strength of year-classes in fish populations due to the amount of suitable prey available during the 'critical period' of larval development (Hjort 1914). Thus, changes in bloom timing could be partly responsible for the yearly fluctuations in the occurrence and abundance of *G. argenteus* observed in the present study, as has been noted for other forage fish species (Régnier et al. 2019). Although spawning habits and the early

life history of the species are beyond the scope of the present study, addressing topics such as spawning areas, duration of yolk sac absorption or development site (planktonic, demersal, etc.) should be the next step towards understanding the response of *G. argenteus* to variations of the current environmental conditions due to climate change.

The spatial effect was the most important variable in the biomass model and explained the second largest deviance in the presence–absence model. The distribution of a species is a complex phenomenon where is not always possible to determine all the drivers (both abiotic and biological) behind the observed spatial effect. For example, the different geomorphologic and oceanographic characteristics between the Galician and Cantabrian Sea waters (Fernández-Salas et al. 2015, Hernández-Molina et al. 2015) could be shaping *G. argenteus*' spatial distribution. Thus, when larvae of *G. argenteus* are present in the study area (Izeta 1985), the eastward shelf-slope Navidad current is still acting (Somavilla et al. 2013). As was observed for several demersal fish species in the area, a low-moderate influx of water of the Navidad current over the progressively narrow shelf of the Cantabrian Sea is necessary to allow eggs and larvae to remain close to nursery areas and not to be transported away to open sea (Sánchez et al. 2001). In addition, the presence of mesoscale anomalies, 'eddies', over the shelf and moving west would enhance recruitment, since these features appear to retain the larvae and juveniles and favour the feeding behaviour of recruits (Sánchez & Gil 2000). According to those authors, topographic factors enhance the effect of the eddies. Hence, the larger continental shelf and the orographic features of the western part may be responsible for the higher abundance of *G. argenteus* observed in this area in most years.

Likewise, it is worth noting the role that dataset resolution has played in the analysis. Chl *a* data for the whole period (1998–2019) was only available at a coarse resolution (22 × 22 km). In our first approach, the spatial effect was included but not year by year and the effects of chl *a* mean concentration and anomaly were significant for both models. Unfortunately, with this approach, a significant spatial autocorrelation in residuals was observed. The spatial autocorrelation was solved by including the spatial effect by year, but during the process, the significant effect of the chl *a* anomaly in the presences–absence model was lost. Thus, it seems that the spatial effect could be, at least partially, masking the effect of the chl *a* anomaly in the distribution of *G. argenteus*. The use of environmental data at a spatial resolution that at

least matches the scale of a species' response to the environment is desirable (although not always possible) for a more reliable estimate of the variable effect and its importance in the model (Mertes & Jetz 2018).

Interestingly, the main aggregation areas for *G. argenteus* located in the present study are quite similar to the commercial fishing trawling effort distribution in the area (e.g. González-Irusta et al. 2018). Fishing is the main driver in the dynamics of forage fish of commercial interest (Engelhard et al. 2014). Although it cannot be ruled out that *G. argenteus* may be impacted by commercial trawling bycatch or simply by disturbance, even if it is not retained in the nets, fishing seems to play little role in the population dynamic of the species not only due to its null economic value in the study area but also due to its small size, which probably reduces its catchability by commercial trawlers. Therefore, it seems that the overlap observed between the persistence aggregations and the commercial fishing effort could be the reflection of predator–prey relationships. Thus, the overall distribution of southern silvery pout could be shaping its commercially important fish predators' niche (e.g. hake, megrim) and in turn, defining the distribution of the commercial trawling effort. This has important implications in terms of fishery management, especially in the current context of climate change, since future modifications in the environmental conditions which favour the observed aggregations could eventually have an impact on the distribution of this prey species and therefore on these predator species of commercially importance and eventually in the fishery.

Our approach has shown that the spatial distribution of *G. argenteus* is influenced by both biotic and abiotic factors. This information is important in improving the understanding of the relationship between environmental factors and *G. argenteus* dynamics in the study area. Such knowledge contributes to a better evaluation of the population status and sheds light on the ecological preferences of a key species in the marine food web of the northern Spanish continental shelf. However, and despite the results obtained in the present study, our understanding of the dynamic ecology of *G. argenteus* is still very limited. Obtaining knowledge on the spawning habits and early life history of the species are an essential requirement for the improvement of future models. In addition, further studies on the species should delve into the link between commercial fishing trawling effort distribution and *G. argenteus* aggregations showed in this work, with the aim of better understanding the relevance of *G. argenteus* in the demersal ecosystem of the southern Bay of Biscay.

LITERATURE CITED

Allouche O, Tsoar A, Kadmon R (2006) Assessing the accuracy of species distribution models: prevalence, kappa and the true skill statistic (TSS). J Appl Ecol 43:1223–1232

Bailey KM, Ciannelli L, Hunsicker M, Rindorf A and others (2010) Comparative analysis of marine ecosystems: workshop on predator–prey interactions. Biol Lett 6:579–581

Barry SC, Welsh AH (2002) Generalized additive modelling and zero inflated count data. Ecol Modell 157:179–188

Bartoń K (2020) MuMIn: multi-model inference. R package version 1.43.17. https://cran.r-project.org/package=MuMIn

Bivand RS, Pebesma E, Gomez-Rubio V (2013) Applied spatial data analysis with R, 2nd edn. Springer, New York, NY

Brackenridge RE, Stow DAV, Hernández-Molina FJ, Jones C and others (2018) Textural characteristics and facies of sand-rich contourite depositional systems. Sedimentology 65:2223–2252

Canty A, Ripley BD (2021) boot: bootstrap R (S-Plus) functions. R package version 1.3-28. https://CRAN.R-project.org/package=boot

Cohen J (1960) A coefficient of agreement for nominal scales. Educ Psychol Meas 20:37–46

Cohen DM, Inada T, Iwamoto T, Scialabba N (1990) Gadiform fishes of the world (Order Gadiformes). An annotated and illustrated catalogue of cods, hakes, grenadiers and other gadiform fishes known to date. In: FAO (ed) FAO species catalogue, Vol 10. FAO, Rome, p 39–40

Colloca F, Bartolino V, Lasinio GJ, Maiorano L, Sartor P, Ardizzone G (2009) Identifying fish nurseries using density and persistence measures. Mar Ecol Prog Ser 381:287–296

Corrales X, Preciado I, Gascuel D, Lopez de Gamiz-Zearra A and others (2022) Structure and functioning of the Bay of Biscay ecosystem: a trophic modelling approach. Estuar Coast Shelf Sci 264:107658

Damalas D, Maravelias CD, Katsanevakis S, Karageorgis AP, Papaconstantinou C (2010) Seasonal abundance of non-commercial demersal fish in the eastern Mediterranean Sea in relation to hydrographic and sediment characteristics. Estuar Coast Shelf Sci 89:107–118

Dormann CF, Elith J, Bacher S, Buchmann C and others (2013) Collinearity: a review of methods to deal with it and a simulation study evaluating their performance. Ecography 36:27–46

Edwards M, Richardson A (2004) Impact of climate change on marine pelagic phenology and trophic mismatch. Nature 430:881–884

Elith J, Leathwick JR (2009) Species distribution models: ecological explanation and prediction across space and time. Annu Rev Ecol Evol Syst 40:677–697

Engelhard GH, Peck MA, Rindorf A, Smout SC and others (2014) Forage fish, their fisheries, and their predators: Who drives whom? ICES J Mar Sci 71:90–104

Enright SR, Boteler B (2020) The ecosystem approach in international marine environmental law and governance. In: O'Higgins TGO, Lago M, DeWitt TH (eds) Ecosystem-based management, ecosystem services and aquatic biodiversity. Springer, Cham, p 333–352

Fernandez-Arcaya U, Rotllant G, Ramirez-Llodra E, Recasens L and others (2013) Reproductive biology and recruitment of the deep-sea fish community from the NW Mediterranean continental margin. Prog Oceanogr 118:222–234

Fernández-Salas LM, Durán R, Mendes I, Galparsoro I and others (2015) Shelves of the Iberian Peninsula and the Balearic Islands (I): morphology and sediment types. Bol Geol Min 126:327–376

Feyrer F, Nobriga ML, Sommer TR (2007) Multidecadal trends for three declining fish species: habitat patterns and mechanisms in the San Francisco Estuary, California, USA. Can J Fish Aquat Sci 64:723–734

Fielding A, Bell J (1997) A review of methods for the assessment of prediction errors in conservation presence/absence models. Environ Conserv 24:38–49

Figueiras F, Labarta U, Fernández-Reiriz M (2002) Coastal upwelling, primary production and mussel growth in the Rías Baixas of Galicia. In: Vadstein O, Olsen Y (eds) Sustainable increase of marine harvesting: fundamental mechanisms and new concepts. Developments in hydrobiology, Vol 167. Springer, Dordrecht, p 121–131

Fowler J, Cohen L, Jarvis P (1998) Practical statistics for field biology. Wiley, Chichester

Gaemers PAM, Poulsen JY (2017) Recognition and distribution of two North Atlantic *Gadiculus* species, *G. argenteus* and *G. thori* (Gadidae), based on otolith morphology, larval pigmentation, molecular evidence, morphometrics and meristics. Fishes 2:15

González-Irusta JM, Wright PJ (2016a) Spawning grounds of Atlantic cod (*Gadus morhua*) in the North Sea. ICES J Mar Sci 73:304–315

González-Irusta JM, Wright PJ (2016b) Spawning grounds of haddock (*Melanogrammus aeglefinus*) in the North Sea and west of Scotland. Fish Res 183:180–191

González-Irusta JM, Wright PJ (2017) Spawning grounds of whiting (*Merlangius merlangus*). Fish Res 195:141–151

González-Irusta JM, De la Torriente A, Punzón A, Blanco M, Serrano A (2018) Determining and mapping species sensitivity to trawling impacts: the BEnthos Sensitivity Index to Trawling Operations (BESITO). ICES J Mar Sci 75:1710–1721

Guntenspergen GR (2014) Application of threshold concepts in natural resource decision making. Springer, New York, NY

Gutiérrez-Zabala JL, Velasco F, Olaso I (2001) Alimentación de veintiuna especies de peces demersales de la división VIIIc del CIEM: otoños de 1994–1995. Inst Esp Oceanogr Datos Resúm 16:1–66

Hastie TJ, Tibshirani RJ (1990) Generalized additive models. Chapman & Hall, London

Hedger R, Mckenzie E, Heath M, Wright PJ, Scott B, Gallego A, Andrews J (2004) Analysis of the spatial distributions of mature cod (*Gadus morhua*) and haddock (*Melanogrammus aeglefinus*) abundance in the North Sea (1980–1999) using generalised additive models. Fish Res 70:17–25

Hengl T (2019) GSIF: global soil information facilities. https://CRAN.R-project.org/web/packages/GSIF/index.html

Hernández-Molina FJ, Wåhlin A, Bruno M, Ercilla G and others (2015) Oceanographic processes and products around

the Iberian margin: a new multidisciplinary approach. Bol Geol Min 126:279–326

Hijmans RJ (2021) raster: geographic data analysis and modeling. R package version 3.5-11. https://CRAN.R-project.org/package=raster

Hijmans RJ, Phillips S, Leathwick J, Elith J (2020) dismo: species distribution modeling. R package version 1.3-3. https://CRAN.R-project.org/package=dismo

Hinz H, Kaiser MJ, Bergmann M, Rogers SI, Armstrong MJ (2003) Ecological relevance of temporal stability in regional fish catches. J Fish Biol 63:1219–1234

Hislop J, Bergstad OA, Jakobsen T, Sparholt H and others (2015) Cod fishes (Gadidae). In: Heessen HJL, Daan N, Ellis JR (eds) Fish atlas of the Celtic Sea, North Sea, and Baltic Sea. Wageningen Academic Publishers, Wageningen, p 186–188

Hjort J (1914) Fluctuations in the great fisheries of northern Europe viewed in the light of biological research. Rapp P-V Réun Cons Int Explor Mer 20:1–228

Hosmer J, David W, Lemeshow S, Sturdivant RX (2013) Applied logistic regression, 3rd edn. John Wiley & Sons, Hoboken, NJ

Houghton RG (1987) The consistency of the spatial distributions of young gadoids with time. ICES Doc CM1987/D:15

Howes GJ (1991) Biogeography of gadoid fishes. J Biogeogr 18:595–622

Husson B, Certain G, Filin A, Planque B (2020) Suitable habitats of fish species in the Barents Sea. Fish Oceanogr 29:526–540

ICES (2017) Manual of the IBTS North Eastern Atlantic Surveys. Ser ICES Surv Protoc SISP 15:1–92

Izeta LM (1985) The larval development of the southern silvery pout *Gadiculus argenteus argenteus* Guichenot (1850). J Plankton Res 7:937–946

Landis JR, Koch GG (1977) The measurement of observer agreement for categorical data. Biometrics 33:159–174

Lindegren M, Van Deurs M, MacKenzie BR, Worsoe Clausen L, Christensen A, Rindorf A (2018) Productivity and recovery of forage fish under climate change and fishing: North Sea sandeel as a case study. Fish Oceanogr 27:212–221

Lindley JA (1977) Continuous plankton records: the distribution of the Euphausiacea (Crustacea: Malacostraca) in the North Atlantic and the North Sea, 1966–1967. J Biogeogr 4:121–133

Longhurst A, Sathyendranath S, Platt T, Caverhill C (1995) An estimate of global primary production in the ocean from satellite radiometer data. J Plankton Res 17:1245–1271

Loots C, Vaz S, Planque B, Koubbi P (2011) Understanding what controls the spawning distribution of North Sea whiting (*Merlangius merlangus*) using a multi-model approach. Fish Oceanogr 20:18–31

López-Jamar E, Cal RM, Gonzalez G, Hanson RB, Rey J, Santiago G, Tenore KR (1992) Upwelling and outwellin effects on the benthic regime of the continental shelf off Galicia, NW Spain. J Mar Res 50:465–488

Lopez-Lopez L, Preciado I, Muñoz I, Decima M, Molinero JC, Tel E (2017) Does upwelling intensity influence feeding habits and trophic position of planktivorous fish? Deep-Sea Res I 22:29–40

Lynam CP, Llope M, Möllmann C, Helaouët P, Bayliss-Brown GA, Stenseth NC (2017) Interaction between top-down and bottom-up control in marine food webs. Proc Natl Acad Sci USA 114:1952–1957

Maravelias CD, Tsitsika EV, Papaconstantinou C (2007) Environmental influences on the spatial distribution of European hake (*Merluccius merluccius*) and red mullet (*Mullus barbatus*) in the Mediterranean. Ecol Res 22:678–685

Mauchline J, Gordon J (1991) Oceanic pelagic prey of benthopelagic fish in the benthic boundary layer of a marginal oceanic region. Mar Ecol Prog Ser 74:109–115

Mbaye B, Doniol-Valcroze T, Brosset P, Castonguay M and others (2020) Modelling Atlantic mackerel spawning habitat suitability and its future distribution in the northwest Atlantic. Fish Oceanogr 29:84–99

Mertes K, Jetz W (2018) Disentangling scale dependencies in species environmental niches and distributions. Ecography 41:1604–1615

Meyer H, Reudenbach C, Hengl T, Katurji M, Nauss T (2018) Improving performance of spatio-temporal machine learning models using forward feature selection and target-oriented validation. Environ Model Softw 101:1–9

Pallaoro A, Jardas I (2002) Remarks on horizontal and vertical distribution of family Gadidae, Lotidae and Phycidae representatives in the eastern Adriatic. Acta Adriat 43:3–15

Pereira JJ, Schultz ET, Auster PJ (2014) Geospatial analysis of habitat use by silver hake *Merluccius bilinearis* in the Gulf of Maine. Endang Species Res 23:219–227

Petitgas P (1998) Biomass-dependent dynamics of fish spatial distributions characterized by geostatistical aggregation curves. ICES J Mar Sci 55:443–453

Planque B, Loots C, Petitgas P, Lindstrøm U, Vaz S (2011) Understanding what controls the spatial distribution of fish populations using a multi-model approach. Fish Oceanogr 20:1–17

Preciado I, Velasco F, Olaso I (2008) The role of pelagic fish as forage for the demersal fish community in the southern Bay of Biscay. J Mar Syst 72:407–417

Preciado I, Punzón A, Velasco F (2015) Spatio-temporal variability in the cannibalistic behaviour of European hake *Merluccius merluccius*: the influence of recruit abundance and prey availability. J Fish Biol 86:1319–1334

R Core Team (2020) R: a language and environment for statistical computing. R Foundation for Statistical Computing, Vienna

Régnier T, Gibb FM, Wright PJ (2019) Understanding temperature effects on recruitment in the context of trophic mismatch. Sci Rep 9:15179

Rey J, Medialdea T (1989) Los sedimentos cuaternarios superficiales del margen continental español. Publ Espec Inst Esp Oceanogr 3:1–30

Roberts DR, Bahn V, Ciuti S, Boyce MS and others (2017) Cross-validation strategies for data with temporal, spatial, hierarchical, or phylogenetic structure. Ecography 40:913–929

Rodríguez-Cabello C, Modica L, Velasco F, Sánchez F, Olaso I (2014) The role of silvery pout (*Gadiculus argenteus*) as forage prey in the Galician and Cantabrian Sea ecosystem (NE Atlantic) in the last two decades. J Exp Mar Biol Ecol 461:193–200

Rueda L, Massutí E, Alvarez-Berastegui D, Hidalgo M (2015) Effect of intra-specific competition, surface chlorophyll and fishing on spatial variation of gadoid's body condition. Ecosphere 6:175

Sagarese SR, Frisk MG, Cerrato RM, Sosebee KA, Musick JA, Rag PJ (2014) Application of generalized additive models to examine ontogenetic and seasonal distribu-

tions of spiny dogfish (*Squalus acanthias*) in the North-east (US) shelf large marine ecosystem. Can J Fish Aquat Sci 71:847–877

Sánchez F (1993) Las comunidades de peces de la plataforma del Cantábrico. Publ Espec Inst Esp Oceanogr 13:1–137

Sánchez F, Gil J (2000) Hydrographic mesoscale structures and Poleward Current as a determinant of hake (*Merluccius merluccius*) recruitment in southern Bay of Biscay. ICES J Mar Sci 57:152–170

Sánchez F, Olaso I (2004) Effects of fisheries on the Cantabrian Sea shelf ecosystem. Ecol Modell 172:151–174

Sánchez F, Serrano A (2003) Variability of groundfish communities of the Cantabrian Sea during the 1990s. ICES Mar Sci Symp 219:249–260

Sánchez F, Gil J, Sánchez R, Mahe JC, Moguedet P (2001) Links between demersal species distribution pattern and hydrographic structures in the Bay of Biscay and Celtic Sea. In: IFREMER (ed) Océanographie du golfe de Gascogne. VII Colloq Int. Actes Colloq 31:173–180

Somavilla R, González-Pola C, Lavín A, Rodríguez C (2013) Temperature and salinity variability in the south-eastern corner of the Bay of Biscay (NE Atlantic). J Mar Syst 109–110(Suppl):S105–S120

Somavilla R, González-Pola C, Fernández-Diaz J (2017) The warmer the ocean surface, the shallower the mixed layer. How much of this is true? J Geophys Res Oceans 122: 7698–7716

Somavilla R, Rodríguez C, Lavín A, Viloria A, Marcos E, Cano D (2019) Atmospheric control of deep chlorophyll maximum development. Geosciences (Basel) 9:178

Tamdrari H, Castonguay M, Brêthes JC, Duplisea D (2010) Density-independent and -dependent habitat selection of Atlantic cod (*Gadus morhua*) based on geostatistical aggregation curves in the northern Gulf of St Lawrence. ICES J Mar Sci 67:1676–1686

Valavi R, Elith J, Lahoz-Monfort J, Guillera-Arroita G (2019) blockCV: an R package for generating spatially or environmentally separated folds for *k*-fold cross-validation of species distribution models. Methods Ecol Evol 10: 225–232

Van der Lingen C, Bertrand A, Bode A, Brodeur R and others (2009) Trophic dynamics. In: Checkley D, Alheit J, Oozeki Y, Roy C (eds) Climate change and small pelagic fish. Cambridge University Press, Cambridge, p 112–157

VanDerWal J, Falconi L, Januchowski S, Shoo L, Storlie C (2014) SDMTools: species distribution modelling tools: tools for processing data associated with species distribution modelling exercises. R package version 1.1-221. https://CRAN.R-project.org/package=SDMTools

Wooster WS, Bakun A, McLain DR (1976) Seasonal upwelling cycle along the eastern boundary of the North Atlantic. J Mar Res 34:131–141

Zhang L, Liu S, Sun P, Wang T, Wang G, Zhang X, Wang L (2015) Consensus forecasting of species distributions: the effects of niche model performance and niche properties. PLOS ONE 10:e0120056

Zuur AF, Ieno EN, Walker NJ, Saveliev AA, Smith G (2009) Mixed effects models and extensions in ecology with R. Springer, New York, NY